

Master thesis on Brain and Cognition
Universitat Pompeu Fabra

A directional view of the Default Mode Network during fMRI resting state and its relation to Episodic Memory

Cabello Toscano, María del Rocío

Supervisor: Deco, Gustavo

Co-Supervisor: Macià Bros, Dídac

6 of July 2020



Contents

| | | |
|----------|---|-----------|
| 1 | Introduction | 1 |
| 2 | Methods | 5 |
| 2.1 | Participants | 5 |
| 2.2 | Neuropsychological Assessment | 6 |
| 2.3 | Functional Magnetic Resonance Images | 6 |
| 2.3.1 | Preprocessing | 7 |
| 2.4 | Parcellations and Time Series Extraction | 7 |
| 2.5 | Normalized Directed Transfer Entropy (NDTE) | 8 |
| 2.6 | Information flow analyses | 10 |
| 2.6.1 | Incoming and outgoing flow | 10 |
| 2.6.2 | Networks definition | 11 |
| 2.6.3 | Group and subject-level analyses | 11 |
| 3 | Results | 13 |
| 3.1 | Information flows | 13 |
| 3.1.1 | Whole cortex | 13 |
| 3.1.2 | DMN | 13 |
| 3.2 | Correlation between Causal Connectivity and Episodic Memory | 14 |
| 3.2.1 | Whole Cortex | 14 |
| 3.2.2 | Within DMN | 15 |
| 3.2.3 | Outside DMN | 16 |

| | |
|----------------------------------|-----------|
| 4 Discussion | 18 |
| 4.1 Discussion | 18 |
| 4.2 Conclusions | 20 |
| References | 22 |
| Statement of contribution | 24 |

Dedication

I would like to dedicate this work to my favorite brother in the world, who have kept me feeling at home during confinement and the whole master's period. He is responsible for having avoided that I spent doing this study more hours than advised to preserve the health.

Acknowledgement

I would like to express my most sincere gratitude to:

- My supervisor and co-supervisor, for trusting me and sharing with me all their knowledge.
- My family, friends and master colleagues, for their daily emotional support, even from the distance.
- All fellows and staff at BBHI and BBSLab, for giving me the opportunity to work with them in this insightful project.

Abstract

Functional MRI (fMRI) and its consequent resting state networks (RSN) have been widely studied from a functional connectivity (FC) perspective. However, FC metrics have not into account statistical temporal dependencies between fMRI signals, which could be describing causal connectivity and hierarchical relations between cortical regions. In order to study this phenomena, a recently published information theoretical statistical criterion (Normalized Directed Transfer Entropy, NDTE) was applied here to analyze the direction underlying information flowing between predefined cortical regions and particularly those forming the well-known Default Mode Network. Participants were 254 healthy middle aged subjects from the outgoing prospective longitudinal study Barcelona Brain Health Initiative (BBHI). BBHI has the goal of analyzing determinants of brain health and so this study has. Episodic Memory (EM) maintenance takes part into successful memory aging and thus scores from the Rey Auditory Verbal Test (RAVLT) were used here to try to find causal connectivity patterns at rest implicated in EM, both in the whole cortex and in the DMN. In general, results showed a hierarchical aspect underlying DMN interactions, along with an inverse correlation between immediate and deferred EM, and the amount of information sent or received by particular regions of the DMN and the whole cortex.

Keywords: Resting State; Functional Magnetic Resonance; Episodic Memory; Causal Connectivity; Default Mode Network

1|Introduction

Networks are present in much more aspects of our lives than we are normally aware of. Without going any further, the system allowing each of us to be aware, among many other cognitive functions, can be studied at different levels of depth as a complex network: the brain. The brain and its ability to produce cognition and behavior has been widely studied in terms of networks (i.e. graph theory) (Sporns, 2018). The brain network could be seen as a composition of cortical regions (i.e. Regions of Interest, ROIs), a set of nodes interconnected by information flow (i.e. network edges). This is the point of view that have been taken in this study. Once the nodes of the network have been defined, the relationship between them has to be measured. Thus, a central question behind this type of studies is how to analyze interactions within the brain connectome. This question has two aspects: *what* (i.e. from what empirical data) and *how* (i.e. with which computational technique).

On the *what* aspect, many different neuroimaging techniques can be used to obtain information about brain connectivity, such as electroencephalography (EEG) or functional magnetic resonance (fMRI). The latter has been very popular in recent years, specially its resting-state version (Farahani, Karwowski, & Lighthall, 2019) (a version discussed here a bit later). fMRI makes use of physical properties such as magnetism and resonance to capture the brain tissue's hemodynamic response. This signal is known as blood-oxygen-level-dependent (BOLD). The idea of comparing BOLD signal with neural signal derives from neuron's necessity of blood supply in obtaining oxygen to optimally operate (Huettel, McCarthy, & Song, 2008). Because of this same reason, this technique has been sometimes very criticized. Some have doubted to which extent hemodynamic activity can be directly understood as

neural activity. Nevertheless there are numerous studies analyzing this relationship with the aim of knowing fMRI's validity. Between all of them, some have found that, when removed the abundant physiological noise, there are correlations between BOLD signal and EEG signal (Birn, 2012). As for EEG, it measures directly electrical activity between neurons, but has a poorer spatial resolution in comparison to fMRI. Therefore, if BOLD signal contains information correlated to these electrical signals, we could talk about brain activity captured by fMRI in a great spatial resolution and in a totally non-invasive way.

There are two conditions in which fMRI can be acquired: resting-state and task-related. Resting-state fMRI, as already mentioned, has been widely studied. It consists on the acquisition of fMRI while the subject is asked to remain still, without thinking about anything in particular. The only main variant among fMRI acquisitions (in terms of experimental design) is whether subjects maintain their eyes closed or not. Despite the simplicity of this paradigm, which is also an advantage in order to repeat experiments because the set-up is easy, it has provided a lot of information about brain connectivity in clinical and non-clinical fields. All in all: rsfMRI poses a highly appropriate technique to study brain connectivity and was the chosen for this study.

On the *how* aspect of analyzing brain connectivity, fMRI has been widely used to measure the interaction and synchrony between cortex regions. To do so, it has been remarkable the analysis of what is known as functional connectivity (FC). FC measures coupling between ROI/voxel's signal with different techniques: Pearson's correlation, frequency coherence, transfer entropy, ordinal correlation and so on. As mentioned before, the resting-state version of fMRI has been very common and so it is the resting-state version of FC (rsFC). Under the study of rsFC, the discovery of the well-known large-scale resting state networks (RSN) has been very important. These comprise a finite set of specific coherent patterns on the cortex. Cortical regions comprising them are highly functionally connected at rest (i.e. high rsFC between each other) (Smitha et al., 2017; van den Heuvel & Hulshoff Pol, 2010). Along with these RSNs, all the studies based on FC are from the perspective of

temporal synchrony, ignoring the possibility that signal in a region could precede or proceed in time the signal in another region. These interactions have been normally studied under the name of effective connectivity (EC) or causal connectivity. RSN have been also analyzed in terms of EC (e.g. (Sharaev, Zavyalova, Ushakov, Kartashov, & Velichkovsky, 2016)), although in a much lower extent than rsFC. Summarizing and in terms of graph theory, it can be said that FC quantifies the connectivity degree of a weighted undirected graph, while EC does it of a weighted directed graph. The directionality added causal connectivity requires seeing the problem from a different point of view in which time has a role. By adding a temporal lag, it is possible to see whether the signal in a region is causing the signal in another region or not, and quantify this interaction. Thus, brain connectivity could be analyzed in terms of hierarchy or directed information flows. In this study, a recently published information theoretical statistical criterion, Normalized Directed Transfer Entropy (NDTE), was used to quantify these causal interactions.

This study is framed in the Barcelona Brain Health Initiative (BBHI), an ongoing prospective longitudinal study committed, as its name indicates, to analyzing determinants of brain health (Cattaneo et al., 2018). In consequence BBHI is interested in successful memory aging among many factors defining brain health. Episodic memory (EM) is one of the most commonly declined functions in unsuccessful memory aging conditions and refers to the ability to recall experienced episodes. Its decline has been shown to become significantly greater around the age of 60 years old, although it seem to be detectable years before (Nyberg & Pudas, 2019). BBHI population (approximately ranging from 45 to 65 years old) is on the border of this range, and hence present a great opportunity to analyze EM just before of its expected decline. In addition, EM has been already found to be affected by connectivity in one particular RSN: the Default Mode Network (DMN). Although changes in DMN connectivity has been already correlated to EM (Huo, Li, Wang, Zheng, & Li, 2018), this has not been done by comparing Causal Connectivity but just rsFC.

By using a time-directed connectivity approach over fMRI data, we wanted to analyze brain activity through the cortex and in particular among DMN regions. In

addition, we aimed to study how much the brain at rest can tell us about EM in a pre-decliners group of healthy people in terms of directed information flows.

2|Methods

2.1 Participants

All data analysed in this study come from the ongoing prospective longitudinal study named Barcelona Brain Health Initiative (BBHI)(Cattaneo et al., 2018), which is focused on identifying determinants of brain health. In the second phase of this study, a sub-cohort of 1000 participants were evaluated through different multi-day in-person assessments. All of them were voluntaries and received no monetary compensation. 254 subjects from the mentioned sub-cohort were randomly chosen in order to use part of their neuroimaging and neuropsychological assessments as the data set analyzed in this master thesis.

All the participants were healthy, with no psychological nor neurological diseases diagnosed, and their age ranged from 43 to 67 in the moment of assessment. Find a brief description of participant’s age and gender in table 1.

| | | Women | Men | Total | |
|--------------|---------|-------|-------|-------|--------------|
| Participants | N | 121 | 133 | 254 | p-value>0.05 |
| | % | 47.64 | 52.36 | 100 | |
| Age (years) | min-max | 43-67 | | 43-67 | |
| | mean | 55.15 | 54.17 | 54.63 | |
| | sd | 7.01 | 6.81 | 6.93 | |

Table 1: Age and gender of the randomly chosen set of subjects. A one-way ANOVA test was run to test the effect of gender in the participant’s distribution of age. As specified, there are no significant differences in age because of gender.

2.2 Neuropsychological Assessment

Among all tests belonging to the neuropsychological evaluation battery from BBHI, we were interested only in the Rey Auditory Verbal Learning Test (RAVLT). This measures the ability that the subject have to recall recent information (in a listened-word format), in two conditions: immediate and deferred.

Firstly the subject listened to the recitation of 15 words and is asked to recall the maximum amount of words he is able to. This is consecutively repeated five times, maintaining the same list of words. Consecutively, a pause of 30 minutes is given to the subject. After it, for the last time he/she is asked to recall words from the list. It is important the fact that the subject has not been warned about being asked about these words again. Then, immediate and deferred scores are calculated based on the amount of recalled words in the first part (i.e. before the 30-minutes pause; immediate memory) and in the second part (i.e. after the 30-minutes pause; deferred memory).

Since RAVLT is measuring the ability of learning/recalling experienced episodes (i.e. having listened to a list of words), this test is used to study Episodic Memory.

2.3 Functional Magnetic Resonance Images

The clinical evaluation of BBHI-participants included Magnetic Resonance Imaging (MRI). These data was acquired with a 3 Tesla Siemens PRISMA scanner and a 32-channel head coil. The MRI session took around one hour and included accelerated multi-band sequences adapted from the Human Connectome Project and provided by the Center of Magnetic Resonance Research (CMRR) at the University of Minnesota. The protocol included different high resolution MR Images. Among them and of our interest, high resolution resting state functional MRI (fMRI) was acquired with spatial resolution of 2x2x2mm and temporal resolution of 0.8 s. Additionally, structural T1- and T2-weighted images were required for preprocessing fMRI data (Cattaneo et al., 2018).

2.3.1 Preprocessing

The preprocessing pipeline made use of functions from FMRIB Software Library (FSL), FreeSurfer and Statistical Parametric Mapping (SPM). To start with, the first 10 scans were removed to ensure magnetization equilibrium. After that, all BOLD images were field inhomogeneity corrected (FSL TopUp) and standardized into native T1-weighted space (SPM Coregister). For nuisance correction, signals from white matter and cerebrospinal fluid (CSF) were extracted and considered as nuisance regressors. Other regressors were those correspondent to motion and to a drift of low frequency oscillations. Motion regressors were 12; six were those of rotation and translation and the other six were their first derivative. The drift was estimated by a discrete cosine transform (DCT) as a low-pass frequency filter (<0.01). All these regressors were regressed out using the FSL function `fsl_regfilt`. Finally, cortical and subcortical segmentation and registration to FreeSurfer standard space (`fsaverage`) was performed in order to being able to compare subjects' fMRI data.

2.4 Parcellations and Time Series Extraction

In order to obtain the set of ROIs in the cortex to be analyzed in this study, we made use of two existent cortical atlases: *HCP-MMP1.0* and *Yeo7*.

The *HCP-MMP1.0* atlas is referred here as *Glasser360*. This atlas consists in 360 cortical Regions of Interest (ROIs), obtained by using multi-modal MRI from the Human Connectome Project (HCP) and taking into account changes in cortical architecture, function, connectivity, and/or topography (Glasser et al., 2016). This atlas was used here to study, in a very precise spatial detail, causal connectivity on the whole cortex and on a particular RSN (i.e. DMN).

On the contrary, the *Yeo* atlas is not that spatially precise. It splits the cortex into 7 or 14 networks (i.e. group of ROIs) according to their rsFC (Yeo et al., 2011). In our study we focused on the version with 7-networks, since one of these can be seen as the one we are interested in (i.e. DMN).

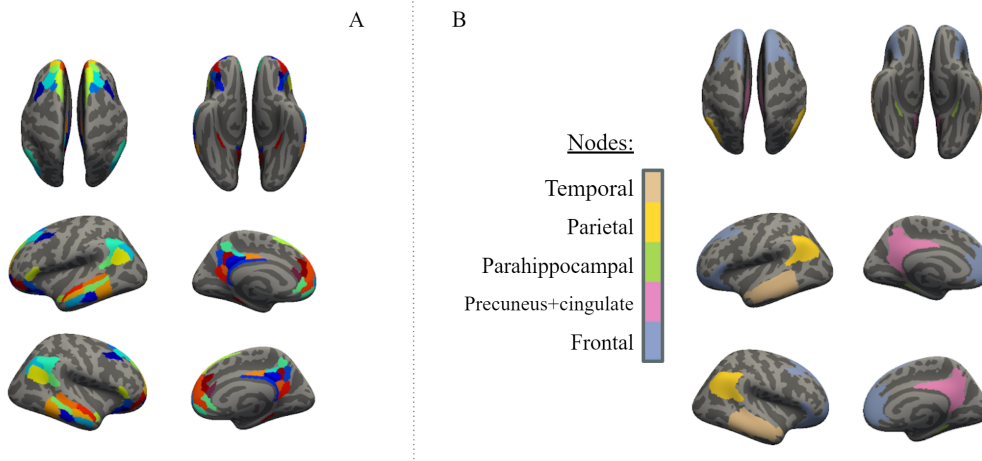


Figure 1: DMN-limited atlas, result of combining Glasser360 and Yeo-7 networks. (A) This DMN-limited atlas is composed by 88 regions from Glasser360. Here these regions are randomly colored. (B) Regions grouped by five network nodes.

As we wanted to study in further detail causal connectivity in the mentioned DMN, a custom-made atlas was created as the intersection between Glasser360 and the DMN-Yeo network. One ROI among the 360 ROIs was considered as part of the new DMN-limited atlas when most of its voxels belong to the corresponding Yeo ROI. This resulted in a set of 88 regions (44 per hemisphere) grouped by five DMN-nodes: *temporal*, *parietal*, *parahippocampal*, *precuneus+cingulate* and *frontal* (see figure 1).

Summarizing, in this study two parcellations were used to extract the cortical BOLD signal of each participant. These two were i) a whole cortex atlas, Glasser360, and ii) a DMN-limited atlas. Both have the same spatial precision as they share 88 Glasser360 regions and the signal extracted per each region was the mean across all the voxels forming the region.

2.5 Normalized Directed Transfer Entropy (NDTE)

We aimed to analyze the directionality of the connectivity between brain regions. This directionality can be seen as the direction in which information is flowing between regions. To analyze this, we compared BOLD signals from different brain regions. BOLD signals can be seen as time-series, consequently we used the time

dimension to make a distinction between past/present signal, and future signal, by adding a temporal lag. In this way we can detect if the past/present of a region, X , is helping to predict the future of another region, Y . Which means that if there is information flowing from X to Y , the past of X would be helping to predict the future of Y (i.e. applying the concept of Granger Causality (Granger, 1969)). Note that adding this temporal lag, and thus comparing past and future of different region's signals, it is what makes it possible to analyze directionality (i.e. from X to Y , and from Y to X).

In order to measure this phenomenon, we used an information theoretical statistical criterion, which was introduced by (Deco, Vidaurre, & Kringelbach, 2019) as Normalized Directed Transfer Entropy (NDTE). The NDTE from a region X to another region Y can be mathematically expressed as:

$$NDTE_{X \rightarrow Y} = \frac{I(Y_{i+1}; X^i | Y^i)}{I(Y_{i+1}; X^i, Y^i)}. \quad (2.1)$$

In the numerator, $I(Y_{i+1}; X^i | Y^i)$ is the mutual information between the future of the region Y (i.e. Y_{i+1}) and the past and present of the region X (i.e. X^i). Note that the past and present signals are denoted by i , which represent all the temporal values in a range $i - T$ (i.e. the temporal lag). This mutual information can be framed in terms of Information Theory. Also known as Transfer Entropy, it measures the degree of statistical dependency between two random variables and can be estimated as a difference of Shannon's Entropies:

$$I(Y_{i+1}; X^i | Y^i) = H(Y_{i+1} | Y^i) - H(Y_{i+1} | X^i, Y^i), \quad (2.2)$$

These entropies, denoted here by H , measure the amount of uncertainty in a random variable given other variable (e.g. $H(Y_{i+1} | X^i, Y^i)$ is the amount of uncertainty in the future of Y given the past of Y and X). In consequence, equation 2.2 describes how much uncertainty is reduced in the future of Y when we additionally know the past of X . If the past of X is not helping to predict Y 's future, then there will be

no change of uncertainty by knowing X and $NDTE_{X \rightarrow Y}$ would be zero.

In the denominator of equation 2.1, $I(Y_{i+1}; X^i, Y^i)$ is the mutual information between the future of the region Y and the past and present of both region Y and X .

$$I(Y_{i+1}; X^i, Y^i) = I(Y_{i+1}; Y^i) + I(Y_{i+1}; X^i | Y^i), \quad (2.3)$$

The objective of adding this term to the NDTE framework is the one of normalizing the transfer entropy in the numerator, and thus allowing comparison among all the NDTE values obtained from different pairs of region's signals.

Once $NDTE$ is computed, it is necessary to study the significance of the obtained statistic. As in (Deco et al., 2019), we used the circular time shifted surrogates method to compute the p-values of the hypothesis testing. This method was firstly proposed by Quiroga et al, and it is well suited for causality analyses. This method simply consist on moving the m first values of a time-series (e.g. X) to the end of it. Being n the length of the time-series to be shifted, m is a random integer within the range $[0.05n \ 0.95n]$. In the case of applying this to compute the significance of an obtained $NDTE_{X \rightarrow Y}$, we shifted X with a random m_x and Y with a different random m_y , and then calculate the new $NDTE_{X' \rightarrow Y'}$ with the shifted versions of X and Y . We repeated this 100 times for each pair X and Y , and afterwards the p-value of $NDTE_{X \rightarrow Y}$ is calculated about these 100 surrogated values (i.e., null hypothesis) and the original NDTE.

2.6 Information flow analyses

2.6.1 Incoming and outgoing flow

Once we had divided the cortex into the Glasser360 regions, the NDTE framework was applied for each participant to obtain the causal interaction between each pair of regions. This resulted in a matrix, G , of dimensions 360x360 (i.e. causal connectivity

matrix) per subject. Each element of the matrix G_{ij} is understood as the amount of information flowing from region i to region j . Because of this directionality, there is no symmetry in these matrices (i.e. $G_{ij} \neq G_{ji}$), as there is in FC matrices. Thus, if we sum the elements of G horizontally, we obtain the total outgoing information flow (G_{out}) of each i region, and if we sum them vertically, we obtain the total incoming information flow (G_{in}) of each j region. G_{in} and G_{out} are then originally vectors of length 360. Additionally, if we sum together all 360 elements in those vectors, we obtain the total information flow in the studied network.

2.6.2 Networks definition

These G matrices and their consequent G_{in} and G_{out} vectors were studied under three different conditions. The first and more general is the *whole-cortex* network. This is a fully connected network of the 360 cortical nodes, whose edges are weighted by their causal interactions (G_{ij}). Nevertheless, the remaining two conditions are based on the DMN-limited atlas. As already explained, this atlas is composed by 88 ROIs from Glasser360. Because of this, the remaining conditions are obtained by masking G to only maintain the values of interest to study the DMN. These two ways of analyzing DMN are named *within DMN* and *outside DMN*. Under the *within DMN* condition, we aimed to analyze causal connectivity between all regions forming the DMN (i.e. DMN-limited atlas). Then, this network was composed by 88 fully connected regions (see figure 2-A), this means all possible interactions within DMN regions. Finally, we also wanted to analyze how DMN interact with the rest of the cortex. This is the purpose of the last remaining condition: *outside DMN*. Here, only interactions between DMN regions and regions outside the DMN were taken into account (see figure 2-B).

2.6.3 Group and subject-level analyses

After G , G_{in} and G_{out} have been obtained for every condition and participant, group and subject-level analyses can be performed. At the group-level, G_{in} and G_{out} are transformed z-scores vector. This means that each region's $G_{in/out}$ is, at the group

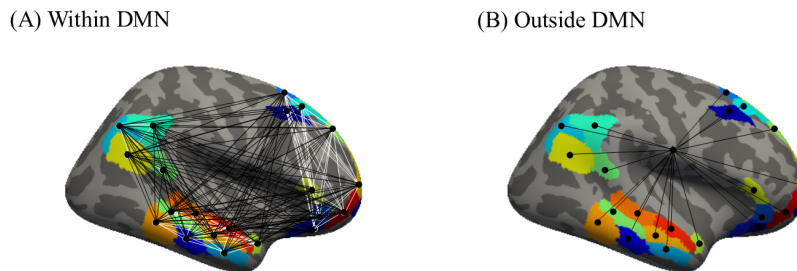


Figure 2: Two possible ways of analyzing DMN. (A) represents intra-DMN interactions, while (B) represents DMN interactions with the rest of the cortex.

level, its mean divided by its standard deviation across subjects. This is done instead of using just the mean operation in order to take into account the variance between subjects. Furthermore, differences between group G_{in} and G_{out} were tested by a one-way t-test.

At the subject-level, our only purpose was to find a correlation between subject's DMN causal connectivity (i.e. G_{in} and G_{out}) and episodic memory. This was done simply by running a Pearson's correlation test between each region's total incoming/outgoing flow (on each of the three conditions) and the two RAVLT scores, and between each total incoming/outgoing flow at the network and the two RAVLT scores. Correlations with age were also analyzed because of its possible effect over these memory scores.

For both types of analyses, statistical results were only considered as significant after correcting their p-values by Bonferroni's Multiple Comparison Correction and these corrected-p-values being lower than 0.05 (i.e. 95% of confidence).

3|Results

3.1 Information flows

3.1.1 Whole cortex

First of all, it was analyzed the direction (i.e. incoming or outgoing) of the information flowing between all possible connections through the cortex. As shown in figure 3, regions that provide the biggest amount of information to the rest of the cortex match with sensory areas and those receiving it to a larger extent are integrative trans-modal areas. These results perfectly fits with results in (Deco et al., 2019), particularly it replicates figure S1 in that paper.

3.1.2 DMN

As shown in figure 4, frontal and parietal DMN nodes are dominants both in relation to other regions in DMN and to the rest of the cortex. These are known to be dominant as significantly result in a negative t value after running a one-way T-test, which was formulated as In minus Out (i.e. negative means $Out > In$ and vice versa). Likewise, parahippocampal nodes are only significantly dominant when delivering information to the rest of the cortex and not within DMN. Regarding temporal and precuneus+cingulate, these nodes are more likely to be receivers in terms of within-DMN interactions. However, these did not showed consistent results regarding node behavior in terms of DMN external communication (i.e. regions in the same node produce information flows in opposite directions; In or Out), in exception to the right temporal node, which seems to be dominant when sending information to

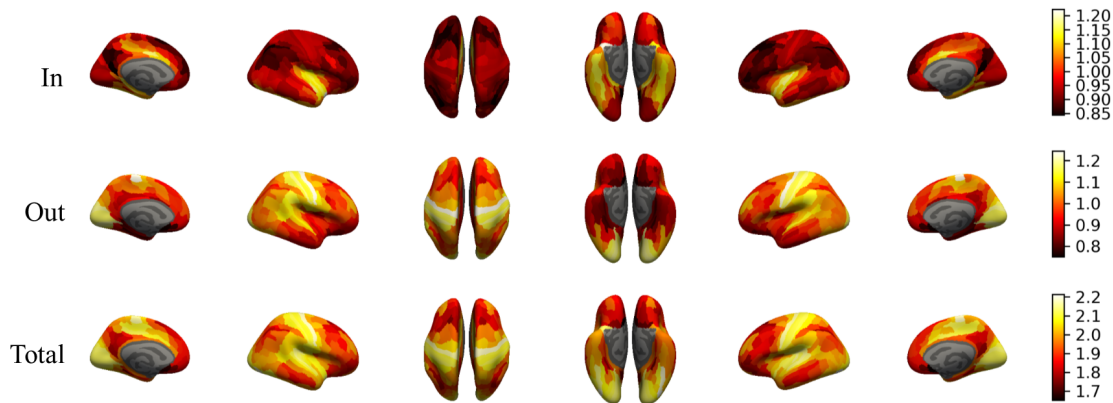


Figure 3: Mean information flowing between all cortical ROIs across subjects, in the two possible directions; incoming and outgoing, and the sum of these two (total).

outside-DMN regions. Inconsistencies about the predominant direction inside the same node also occur in some other nodes (e.g. right frontal node, region p24 or posterior Brodmann area 24) but always on the borders of the node, which possibly represents an overestimation on the node’s spatial definition.

3.2 Correlation between Causal Connectivity and Episodic Memory

3.2.1 Whole Cortex

When analyzing total information flow between whole cortex regions, significant correlations were found between them and age, and immediate memory. Both total incoming and total outgoing showed an inverse effect over immediate memory, with a slightly higher effect of outgoing than incoming. Regarding age, this correlation was direct and only in terms of total incoming. See table 2 for numerical details.

At the region level, there was no significant effect of age but of immediate and deferred memory. All these resulting regions had an inverse correlation between directional information flow and memory scores, with an effect size of around 0.2. Particularly, and as shown in figure 5, part of the left Brodmann area 8 (left 8C), left Lateral Belt Complex (LBelt), right Middle Belt Complex (MBelt) and right Tempo-

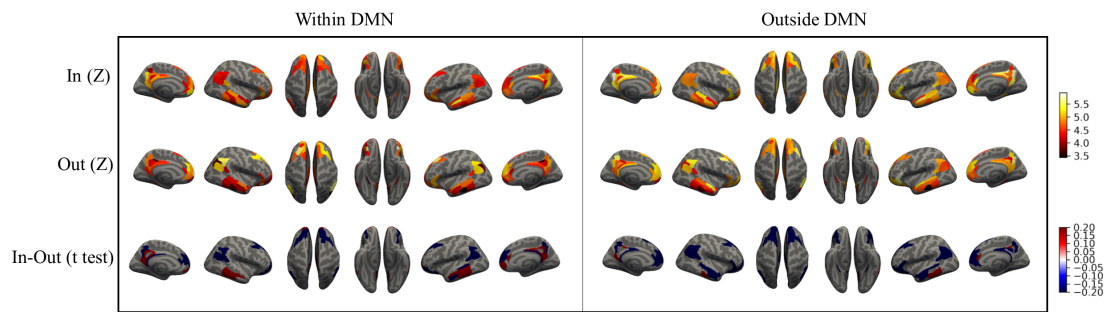


Figure 4: Information flowing between DMN-regions (i.e. *Within DMN*) and between DMN and non-DMN-regions (i.e. *Outside DMN*). *In* and *Out* rows shows the amount of information flowing from/to each region of the network, on average and adjusted by the effect of its standard deviation (Z-score). The bottom row, *In-Out* shows which regions have, on average, a significantly higher amount of Incoming information than Outgoing (i.e. red regions), or vice versa (i.e. blue regions). This effect is plotted by a statistical T-test and only those regions with a p-value < 0.05 are colored in these plots.

ral Area 1 middle (TE1m) exhibited correlation between incoming from other cortex regions and immediate memory. In the case of outgoing to other cortex regions, these correlations were significant in the left Perhinal Ectorhinal cortex (PeEc) and left Brodmann area 43. However, deferred memory only showed correlation to amount of outgoing information and one single region, the left Perhinal Ectorhinal cortex (PeEc). Thus, outgoing information from this region is affecting both immediate and deferred memory.

3.2.2 Within DMN

When analyzing total information flow between DMN regions, no significant correlations were found between them and age, neither between them and memory scores. See table 2 for numerical details.

At the region level, there was no significant effect of age nor deferred memory, but of immediate memory. All resulting regions had an inverse correlation between directional information flow and immediate memory score, with an effect size of around 0.2. Particularly, and as shown in figure 5, these were left and right Temporal Areas 1 middle (TE1m) and right anterior Superior Temporal Gyrus (STGa), which

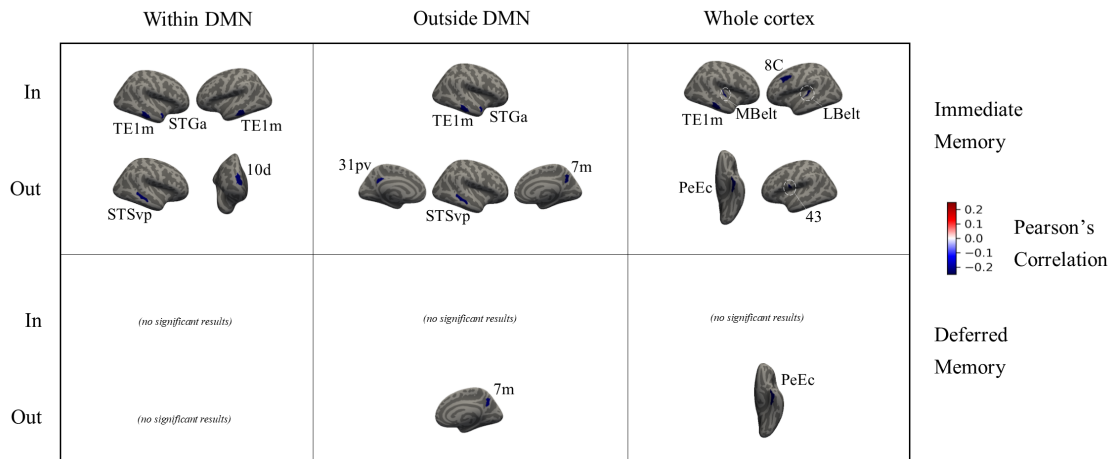


Figure 5: Significant correlations (p -value <0.06 after Bonferroni Correction) between information flowing and RAVLT scores. These come from three different conditions, within DMN interactions, interactions between DMN regions and outside-DMN regions and interactions between whole cortex regions. Significant regions are labelled according to Glasser360 atlas: TE1m, Temporal Areas 1 middle; STGa, Superior Temporal Gyrus anterior; STSvp, Superior Temporal Sulcus ventral posterior; 10d, part of Brodmann area 10; 31pv part of Brodmann area 31, 7m, part of Brodmann area; 8C, part of Brodmann area 8; MBelt, Middle Belt Complex; LBelt, Lateral Belt Complex; PeEc, Perihinal Ectorhinal cortex; 43, Brodmann area 43

exhibited correlation between incoming from other DMN regions and immediate memory. In the case of outgoing to other DMN regions, these correlations were significant in the right Superior Temporal Sulcus ventral posterior (STSvp) and part of the right Brodmann area 10 (10d). All mentioned regions were located within the temporal DMN-node, except for 10d which is in the frontal.

3.2.3 Outside DMN

When analyzing total information flow between DMN regions and other cortical regions, no significant correlations were found between them and age, neither between them and memory scores. See table 2 for numerical details.

At the region level, there was no significant effect of age but of immediate and deferred memory. All these resulting regions had an inverse correlation between directional information flow and memory scores, with an effect size of around 0.2. Particularly, and as shown in figure 5, right Temporal Area 1 middle (TE1m) and

| | | Pearson's Correlation | p-value | p-value<0.05 |
|-------------------------|------------------------------|--------------------------|-----------------|--------------|
| Whole cortex | In vs age | 1.37e-01 | 2.96e-02 | * |
| | Out vs age | 1.05e-01 | 9.36e-02 | |
| | In vs Immediate Mem. | -1.69e-01 | 6.96e-03 | * |
| | Out vs Immediate Mem. | -2.08e-01 | 8.63e-04 | * |
| | In vs Deferred Mem. | -1.04e-01 | 9.68e-02 | |
| | Out vs Deferred Mem. | -1.12e-01 | 7.53e-02 | |
| Within DMN | In vs age | 4.33e-01 | 1.95e-01 | |
| | Out vs age | 1.23e-01 | 2.77e-01 | |
| | In vs Immediate Mem. | 6.60e-02 | 2.17e-01 | |
| | Out vs Immediate Mem. | 2.24e-01 | 2.21e-01 | |
| | In vs Deferred Mem. | 2.41e-01 | 4.65e-01 | |
| | Out vs Deferred Mem. | 1.68e-01 | 1.30e-01 | |
| Outside DMN | In vs age | 2.21e-01 | 1.38e-01 | |
| | Out vs age | 1.38e-01 | 2.24e-01 | |
| | In vs Immediate Mem. | 4.25e-01 | 1.71e-01 | |
| | Out vs Immediate Mem. | 2.25e-01 | 2.85e-01 | |
| | In vs Deferred Mem. | 2.61e-01 | 3.74e-01 | |
| | Out vs Deferred Mem. | 2.05e-01 | 1.41e-01 | |

Table 2: Pearson correlation between age or memory scores (RAVLT) and total information flows in the three studied networks.

right anterior Superior Temporal Gyrus (STGa) exhibited correlation between incoming from other cortex regions and immediate memory. In the case of outgoing to other cortex regions, these correlations were significant in part of the left ventral Brodmann area 31 (31pv), part of the right Brodmann area 7 (7m) and right Superior Temporal Sulcus ventral posterior (STSvp). However, deferred memory only showed correlation to amount of outgoing information and one single region, the same part of the right Brodmann area 7 (7m) that whose outgoing information was also affecting immediate memory.

4|Discussion

4.1 Discussion

In a general way and as it has been already exposed in the result's section, in this study part of the results of Deco et al. (2019) has been replicated. Sensory areas have higher amount of information flowing to the rest of the cortex and integrative areas have higher amount of information flowing into them from the rest of the cortex. This sounds trivial since one of the main goals of the brain is to allow us to constantly communicate with the external world. In doing so, we need to provide our brain with information collected by the senses. Thus, these sensory regions represent, as checked here, a main input of information to the rest of the cortex. After receiving all this external information, it is of no use if we are not able to integrate it. Here integrative areas come into play. These are also expected and seen to receive the biggest amount of information from the rest of the cortex, as can be hypothesized, in the attempt of making sense of information from different modalities together. Having replicated these results allow us to start from a reliable baseline. This help us to trust even more on the results of analyzing a different situation by using this same framework.

Regarding whole-cortex interactions, regions with a significant correlation between information sharing and EM are related to audition (MBelt and LBelt), memory in itself (PeEc), verbal selection (Brodmann Area 43) (Gabrieli, Poldrack, & Desmond, 1998), uncertainty processing (8C) (Volz, Schubotz, & von Cramon, 2005) and non-verbal processing (right TE1m). These seem to be very intuitive results, as RAVLT implies all these functions. Since all these correlations are negative, it could be in-

tuit that less information entering to sensory and processing areas (MBelt, LBelt, 8C and TE1m) and exiting from memory and decision making (PeEc and 43), at rest, lead to better memory in the task. It can not be known from this resting data, but it could be hypothesized an opposite effect while performing the task; i.e. higher information flowing in those directions would lead to better memory performance.

One of the main objectives in this thesis was to study the DMN from a directional point of view. As it has been seen, most of the nodes in the network act as compact nodes despite the variability across subjects. This can be guessed here as they mainly have a particular role in terms of directionality. Within DMN interactions showed that frontal and parietal nodes act as information givers to the rest of the DMN, while precuneus+cingulate and temporal nodes act as information receivers and parahippocampal nodes have a neutral role. At the view of this, we could be talking about a hierarchy underlying DMN at rest. Precuneus area has been seen as a important hub (i.e. information giver) in many other studies such as the already mentioned here Deco et al. (2019). The fact that it has a different role here is contraintuitive and may be caused by the effect of limiting interactions in terms of DMN nodes, but not necessarily means that it has not an important role inside the network. On the other hand, DMN nodes have been widely demonstrated to be functionally connected at rest and disconnected when performing a task. A question that arises but cannot be answered here is whether this hierarchy would also change in the presence of a task.

Although DMN nodes have in general a specific role regarding direction in information sharing, the fact of having a better or worse performance in a EM task is related to concrete and smaller regions inside these nodes (most specially in temporal DMN-nodes). These results were possible because we used a finer parcellation of the DMN by merging Glasser360 and Yeo7. Then, it seems important to study behavior inside DMN-nodes in spatial detail, instead of using a compact-node approach. The same applies to all the other well-known large scale networks. Not doing it like that could lead to false negatives (e.g. no correlation between the studied network, nor part of it, and a particular cognitive aspect or disease).

As shown in the results, DMN regions whose interactions inside the network correlate to immediate memory performance are found mainly in the temporal DMN-node. These regions have a role as information givers inside the network. As commented, mostly all regions in the temporal nodes have this role. Losing this balance in the temporal DMN-nodes in those significant regions (TE1m, STGa and STSvp) makes the subject to have worse or better immediate memory performance. Nevertheless, there is no significant effect of these regions nor any others within DMN over deferred memory.

Here, it could be interesting to remark the bilateral effect of TE1m within DMN. At the view of it, both verbal and non-verbal areas seem to be important for immediate recall performance at RAVLT. This effect disappears when interactions are between DMN and outside-DMN regions, or even between all whole cortex regions. In these cases, there is only effect of the right temporal lobe, indicating no differences in the amount of verbal information sent to the rest of the cortex and no effect of language over memory performance, which seems contraintuitive. Along with these right temporal effects in the outside-DMN condition, precuneus+cingulate nodes come into play. More precisely, one region of each node (i.e. left and right) is affecting immediate memory performance by having a different amount of outgoing information to the rest of the cortex. Regions in these nodes have not an unified role regarding Outside-DMN condition. Finally it seems interesting and again contraintuitive that the hippocampal DMN-nodes have no effect over these memory scores, since it is an important area for memory. However, this could be caused by an insufficient parcellation of the area.

4.2 Conclusions

The main conclusion of this study is that temporal statistical dependencies among BOLD signal can describe very interesting phenomena in terms of brain activity. As it has been shown here, there is an hierarchical aspect underlying DMN interactions. In this hierarchy, frontal and parietal DMN nodes play a temporal dominant role over both the rest DMN nodes and the rest of the cortex, while precuneus+cingulate

and temporal areas are under the dominance of the rest of DMN nodes.

Regarding EM, the causal connectivity perspective taken here is able to reveal directional implications in regions related to functions needed to correctly complete the EM test used here (i.e. RAVLT), such as audition, memory and verbal processing. In addition, it has also revealed changes in the directional role of very spatially precise regions of the DMN (particularly in temporal and precuneus+cingulate areas).

All in all, causal connectivity analyses provide a very potential and not really explored approach to describe cortical interactions and patterns of activity which could improve the understanding about cognition in healthy and clinical paradigms.

References

- Birn, R. M. (2012). The role of physiological noise in resting-state functional connectivity. *NeuroImage*, *62*(2), 864 - 870. Retrieved from <http://www.sciencedirect.com/science/article/pii/S105381191200033X> (20 YEARS OF fMRI) doi: <https://doi.org/10.1016/j.neuroimage.2012.01.016>
- Cattaneo, G., Bartrés-Faz, D., Morris, T. P., Sánchez, J. S., Macià, D., Tarrero, C., ... Pascual-Leone, A. (2018). The barcelona brain health initiative: A cohort study to define and promote determinants of brain health. *Frontiers in Aging Neuroscience*, *10*, 321. Retrieved from <https://www.frontiersin.org/article/10.3389/fnagi.2018.00321> doi: 10.3389/fnagi.2018.00321
- Deco, G., Vidaurre, D., & Kringelbach, M. L. (2019). Revisiting the global workspace: Orchestration of the functional hierarchical organisation of the human brain. *bioRxiv*. Retrieved from <https://www.biorxiv.org/content/early/2019/11/29/859579> doi: 10.1101/859579
- Farahani, F. V., Karwowski, W., & Lighthall, N. R. (2019). Application of graph theory for identifying connectivity patterns in human brain networks: A systematic review. *Frontiers in Neuroscience*, *13*, 585. Retrieved from <https://www.frontiersin.org/article/10.3389/fnins.2019.00585> doi: 10.3389/fnins.2019.00585
- Gabrieli, J. D. E., Poldrack, R. A., & Desmond, J. E. (1998). The role of left prefrontal cortex in language and memory. *Proceedings of the National Academy of Sciences*, *95*(3), 906–913. Retrieved from <https://www.pnas.org/content/95/3/906> doi: 10.1073/pnas.95.3.906
- Glasser, M. F., Coalson, T. S., Robinson, E. C., Hacker, C. D., Harwell, J., Yacoub,

- E., ... et al. (2016). A multi-modal parcellation of human cerebral cortex. *Nature*, *536*(7615), 171–178. doi: 10.1038/nature18933
- Granger, C. W. J. (1969). Investigating causal relations by econometric models and cross-spectral methods. *Econometrica*, *37*(3), 424–438. Retrieved from <http://www.jstor.org/stable/1912791>
- Huettel, S. A., McCarthy, G., & Song, A. W. (2008). *Functional magnetic resonance imaging*. W.H. Freeman.
- Huo, L., Li, R., Wang, P., Zheng, Z., & Li, J. (2018). The default mode network supports episodic memory in cognitively unimpaired elderly individuals: Different contributions to immediate recall and delayed recall. *Frontiers in Aging Neuroscience*, *10*, 6. Retrieved from <https://www.frontiersin.org/article/10.3389/fnagi.2018.00006> doi: 10.3389/fnagi.2018.00006
- Nyberg, L., & Pudas, S. (2019). Successful memory aging. *Annual Review of Psychology*, *70*(1), 219–243. Retrieved from <https://doi.org/10.1146/annurev-psych-010418-103052> (PMID: 29949727) doi: 10.1146/annurev-psych-010418-103052
- Sharaev, M. G., Zavyalova, V. V., Ushakov, V. L., Kartashov, S. I., & Velichkovsky, B. M. (2016). Effective connectivity within the default mode network: Dynamic causal modeling of resting-state fmri data. *Frontiers in Human Neuroscience*, *10*, 14.
- Smitha, K., Raja, K. A., Arun, K., Rajesh, P., Thomas, B., Kapilamoorthy, T., & Kesavadas, C. (2017). Resting state fmri: A review on methods in resting state connectivity analysis and resting state networks. *The Neuroradiology Journal*, *30*(4), 305–317. Retrieved from <https://doi.org/10.1177/1971400917697342> (PMID: 28353416) doi: 10.1177/1971400917697342
- Sporns, O. (2018, 06). Graph theory methods: applications in brain networks. *Dialogues in Clinical Neuroscience*, *20*, 111–121.
- van den Heuvel, M. P., & Hulshoff Pol, H. E. (2010). Exploring the brain network: A review on resting-state fmri functional connectivity. *European Neuropsychopharmacology*, *20*(8), 519 - 534. Retrieved from <http://www.sciencedirect.com/science/article/pii/S0924977X10000684> doi:

<https://doi.org/10.1016/j.euroneuro.2010.03.008>

- Volz, K. G., Schubotz, R. I., & von Cramon, D. Y. (2005). Variants of uncertainty in decision-making and their neural correlates. *Brain Research Bulletin*, *67*(5), 403 - 412. Retrieved from <http://www.sciencedirect.com/science/article/pii/S0361923005002273> (2nd Conference on NeuroEconomics - ConNEcs 2004) doi: <https://doi.org/10.1016/j.brainresbull.2005.06.011>
- Yeo, B. T., Krienen, F., Sepulcre, J., Sabuncu, M., Lashkari, D., Hollinshead, M., ... Buckner, R. (2011, 06). The organization of the human cerebral cortex estimated by functional correlation. *Journal of neurophysiology*, *106*, 1125-65. doi: 10.1152/jn.00338.2011

Statement of contribution

- Conceptualization Ideas: Dídac Macià, Gustavo Deco and BBHI.
- Methodology Development: Gustavo Deco and Dídac Macià.
- Software Programming
 - FMRI Preprocessing: Dídac Macià and María Cabello.
 - Normalized Directed Transfer Entropy: Gustavo Deco.
- Experimental design and data collection: BBHI.
- Formal Analysis Application: María Cabello.
- Visualization Preparation: María Cabello.
- Writing – Original Draft Preparation: María Cabello.